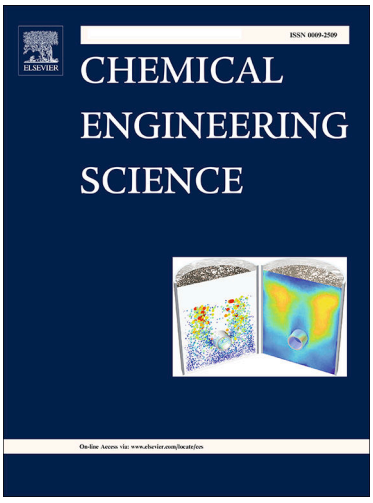

Location optimization of silicon carbide foam packings in the unstirred packing trays re-actor for the enhancement of solidified natural gas storage

Linqing Tian, Li Ha, Li Wang, Guangjin Chen, Frederic Coulon, Yuelu Jiang, Xinyang Zeng, Ruifeng Zhang, Guozhong Wu

PII: S0009-2509(22)00087-2
DOI: https://doi.org/10.1016/j.ces.2022.117503
Reference: CES 117503

To appear in: *Chemical Engineering Science*

Received Date: 2 July 2021
Revised Date: 1 January 2022
Accepted Date: 6 February 2022

Please cite this article as: L. Tian, L. Ha, L. Wang, G. Chen, F. Coulon, Y. Jiang, X. Zeng, R. Zhang, G. Wu,Location optimization of silicon carbide foam packings in the unstirred packing trays reactor for the enhancement ofsolidified natural gas storage, *Chemical Engineering Science* (2022), doi: https://doi.org/10.1016/j.ces.2022.117503

Chemical Engineering Science, Volume 253, May 2022, Article number 117503
DOI: 10.1016/j.ces.2022.117503

Location optimization of silicon carbide foam packings in the unstirred packing trays reactor for the enhancement of solidified natural gas storage

Linqing Tian[1,2], Li Ha[2], Li Wang[2], Guangjin Chen[3], Frederic Coulon[4], Yuelu Jiang[2], Xinyang Zeng[5], Ruifeng Zhang[6], Guozhong Wu[1, 2, *]

[1] Institute of Environmental and Ecological Engineering, Guangdong University of Technology, Guangzhou, 510006, China

[2] Institute of Ocean Engineering, Shenzhen International Graduate School, Tsinghua University, Shenzhen 518055, China

[3] State Key Laboratory of Heavy Oil Processing, China University of Petroleum, Beijing, 102249, China

[4] School of Water, Energy, and Environment, Cranfield University, Cranfield, MK43 0AL, UK

[5] Southern Marine Science and Engineering Guangdong Laboratory (Guangzhou), Guangzhou 511458, China

[6] Shenzhen Qihay Academy Science and Technology Co., Ltd., Shenzhen 518055, China

* Corresponding Author

Email: guozhong2022@hotmail.com

Abstract:

Solidified natural gas technology shows significant potential for storing safely multi-fold volumes of natural gas in clathrate hydrates, but the main concern is the stochastic and slow process of hydrate nucleation making it unstable and unpredictable in practice. To overcome this limitation, methane hydrate was synthesized in a silicon carbide (SiC) ceramic foam packing trays reactor without stirring. Results suggested that the packing trays should be located near the gas-water interface instead of immersed in the aqueous phase, which decreased the induction time by about 98%. Results also highlighted the synergistic effects between the capillary wicking from the porous packings and the water suction from the initially formed hydrate clusters, which pumped water from the aqueous phase into the packings' pores to provide an unsaturated porous environment for hydrate nucleation. It demonstrated that these two driving forces might also compete for water which became adverse to hydrate formation.

Keywords: methane hydrate, SiC foam tray, nucleation, solidified natural gas, gas storage

1. Introduction

Natural gas is a clean energy resource that will account for a quarter of global energy demand by 2040 and will pave the way for the transition from fossil fuels to zero-carbon energy (IEA, 2017). Natural gas can be stored and transported either in the form of compressed gas or liquefied gas. However, recent studies have shown that solid natural gas hydrate (SNG) offers a new cost-effective alternative for gas storage and transportation (Bhattacharjee et al., 2020). For large-scale and long-distance gas transportation, liquefied natural gas (LNG) is the most widly used approach, but the LNG storage requires extreme low temperature (-162°C) and there are safty issues due to the continuous boil-off. By contrast, the gas storage by SNG requires moderate temperature and pressure conditions, which is safer as the gas can be released in a non-explosive manner and it is possible to recover 100% of the stored gas by simple depressurization or minimal thermal stimulation (Veluswamy et al., 2018). However, the hydrate nucleation is a stochastic and slow process, making it difficult to control in practice. For example, the induction time for methane hydrate nucleation is often unstable and vary from a few mininutes to hundreds of mininutes under the same experimental conditions (Liu et al., 2019). One of the chanllenges for the commercial application of the SNG technology is how to rapidly convert natural gas to hydrates with high storage capacity.

Therefore, there are increasing demands for developing approaches to promote hydrate formation by adding porous materials such as sand packs, silica gels, hydrogels, nanoparticles and foam packings (Linga and Clarke, 2017). Recently, a silicon carbide (SiC) foam ceramic (SFC) packing, which is a porous material synthesized by blending

silicon carbide with foamed polyurethane and sintering at 1500-2000°C after curing and drying (Qian and Jin, 2006), was for the first time applied in our laboratory to facilitate hydrate nucleation and enhance the gas storage capacity (Liu et al., 2019). In addition to provide large specific surface area for hydrate nucleation, the application of SFC packings could also effectively remove the hydration heat produced from hydrate formation. For instance, it could decrease the overall thermal resistance by between 38% and 62% in the reaction system and maintain the reaction system at a low thermal resistance under relative low driving force (Tian and Wu, 2020b). These studies demonstrated the role of the stacking patterns of SFC packings on the heat and mass transfer and highlighted the demands for the special design of the reactor structure to support the packings in future works (Liu et al., 2019). It remains however unknown how the hydrate formation kinetics can be influenced by the relative space between the packings as a block of foam packings were always directly placed at the bottom of the reactor in previous studies (Yang et al., 2011; Fan et al., 2012; Babu et al., 2013b; Liu et al., 2019). Further studies are also needed to decipher if and how the relative space between the packings and the gas-water interface would influence the packings' performance, because the thick water layer above the packings provide resistance for the gas to pass through before reaction with the pore water inside the packings (Liu et al., 2019). Accordingly, the concept of plate-type reactor with SiC foam packing tray was used in the present study to address these issues. Such type of reactors had been previously used in other unit operations of chemical engineering (e.g., distillation) to provide better mixing and thus achieve better mass and energy transfer

between liquid and vapor (Zhang et al., 2012; Zhang et al., 2013; Yan et al., 2018).

Another way to facilitate hydrate formation is to add chemical promoters. The most widly used promoter is surfactant such as sodium dodecyl sulfate (SDS), but the large-scale application of SDS may pose environmental risks as it is toxic to aquatic organisms (Messina et al., 2014). Moreover, the usage of surfactants would generate foams which impacted the efficiency of SNG method and cause the loss of surfactants (Wang et al., 2018). Most recently, we employed cyclodextrin-SDS mixture solution to reduce the dosage of SDS by about 67% (Tian and Wu, 2020b). Cyclodextrin was used as it is a non-toxic and environmentally friendly oligosaccharide which has the capability of facilitating the formation of water channel bridging hydrate and water and increasing the gas−water interfacial curvature (Ji et al., 2017). Indeed, the use of cyclodextrin-SDS mixture allowed us to increase the total gas uptake by more than 83% with a 7-fold higher hydrate formation rate (Tian and Wu, 2020b). However, our previous study was performed under mechanical stirring conditions which are not ideal in terms of cost-effectiveness for storage and transportation. Therefore, further work is needed to evaluate whether similar formation rate can be obtained under static (unstirred) conditions for energy savings purpose. This motivated us to combine the cyclodextrin-SDS mixture solutions with the SiC foam tray to enhance hydrate formation. Specific objectives of this study were to (i) optimize the position of SiC foam location by testing the performance of the tray reactor with packings separated by different spaces, and (ii) clarify how and why the performance would vary with the distance between the packings and the gas-water interface.

2. Materials and Methods

Methane (99.99% purity) used in this study was supplied by Shenzhen Huatepeng Co., Ltd. Sodium dodecyl sulfate (SDS, analytical reagent grade, 99 % purity) was purchased from Beijing Bailingwei Chemical Technology Co., Ltd. The α-cyclodextrin (αCD, 98% purity) was purchased from Aladdin Industrial Corporation. The SDS and αCD were dissolved in deionized water and thoroughly mixed for at least 60 min to form mixture solutions. The concentration of SDS and αCD in the mixture solution was 100 and 200 mg L^{-1}, respectively. This was an optimal formulation previously screened from four types of cyclodextrins with different structures and concentrations in the methane hydrate synthesis experiments (Tian and Wu, 2020a), which was therefore directly used in the present study. The SFC packing in the shape of disks (diameter: 45 mm, thickness: 8 mm, pore size: 3 ~ 5 mm, porosity: 60%, mass: 14.1 g) were obtained from the Institute of Metal Research, Chinese Academy of Sciences. As shown in Fig. 1, a stainless-steel reactor internal was tailored by welding six parallel rings to a vertical thin column so that different amount of SFC packings could be located on the rings at different positions.

The methane hydrate formation experiments were carried out in a high pressure reaction system which was described in our previous study (Tian and Wu, 2020a). The hydrate was synthesized in a cylindrical stainless-steel reactor (diameter: 50 mm, height: 80 mm) with the maximum pressure capability of 20 MPa. The reactor was immersed in a circulating coolant bath (268.2 ~ 323.2 K) for temperature control. The temperature and pressure were recorded every 10 s using a temperature transducer (PT-100) and a pressure

transducer (DC1300), respectively.

Before experiments, the high-pressure reactor was washed with deionized water for three times and dried with compressed air. The αCD-SDS mixture solution (40 mL) was added into the reactor, subsequently, the reactor internal with SFC packings loaded in advance was carefully put into the reactor. The reactor was purged with methane gas (0.5 ~ 1.0 MPa) to remove the residual air and pressurized with methane gas to the desired pressure, which was then soaked in the coolant bath. The moment when the reaction system reached the designed temperature (275.4 K) and pressure (8.0 MPa) was recorded as time zero. The hydrate nucleation was recognized when a sharp increase in the temperature and a sudden decrease in the pressure were observed. The methane hydrate formation process was considered completed when the temperature and pressure kept constant for 3 h. Each experiment was repeated for at least three times. The key parameters for characterizing hydrate formation kinetics such as the induction time (T_{ind}, h), methane gas uptake (mol gas mol^{-1} water), maximum formation rate (F_{max}, m^3 gas m^{-3} water min^{-1}) and percentage of water conversion to hydrate (%) were calculated using the obtained gas consumption data according to the methods elaborated in our previous study (Tian and Wu, 2020a).

3. Results and Discussion

Effect of separating distance between two packings on hydrate formation: In order to investigate the influence of the sepatating distance between SFC packings on hydrate formation, we designed three scenarios (Scenario A – C) by locating the bottom SFC packing at the first layer (L_1) while changing the position of the top SFC packing. In Scenario A (Fig. 1a), the top packing was located at the second layer (L_2). The two packings were very close to each other with a distance of ~ 2 mm. In Scenario B (Fig. 1b), the top packing was located at the third layer (L_3) and the distance between the two packings was about 12 mm. In Scenario C (Fig. 1c), the top packing was located at the fourth layer (L_4) and the corresponding distance between packings was 22 mm. In these cases, the mass ratio of packing to water was 70%. In order to provide blank control, experiments were also performed by adding only αCD-SDS mixture solution but not adding the stainless-steel reactor internal and SFC packings. Results indicated that it was insufficient to promote hydrate formation at unstirred conditions using the mixture solution alone as the corresponding gas uptake was almost zero within 48 h when we repeated the blank control experiments for five times (Fig. 2).

In Scenario A, the final gas consumption after reaction was about 122.0 mmol gas mol^{-1} water, the percentage of water conversion to hydrate was 74%, and the maximum formation rate was 6.5 m^3 gas m^{-3} water min^{-1} (Figs. 2 - 4). These three parameters were very close to that obtained in our previous study where methane hydrate was synthesized without SFC packings, but under 600 rpm magnetic stirring conditions using the 200 mg

L^{-1} αCD - 100 mg L^{-1} SDS mixture solution (Tian and Wu, 2020a). This finding demonstrated that the application of SFC packings could trigger the hydrate nucleation. However, the induction time in this case was 22.3 h (Fig. 5), which was about 670 times longer than the results obtained under stirring conditions using the same concentration of αCD-SDS mixture solution (Tian and Wu, 2020a). Therefore, it might not be the best way to enhance gas hydrate formation by directly stacking the packings at the bottom of the reactor as usually did in previou studies.

The hydrate nucleation rate was significantly facilitated after increasing the space between the two packings by moving the top packing from L_2 to L_3. As shown in Fig. 5, the induction time decreased by 36% in Scenario B compared with Scenario A. Nevertheless, the improvement of packings' performance in terms of the hydrate growth rate was relatively slight. For instance, the gas uptake inceased to 128.0 mmol gas mol^{-1} water, the percentage of water conversion to hydrate increased to 78%, while the maximum formation rate increased to 6.9 m^3 gas m^{-3} water min^{-1} in Scenario B (Figs. 2 -4). When the distance between the two packings futher increased to 22 mm (Scenario C), the induction time for methane hydrate nucleation decreased to 6.5 h which was 71% faster than the nucleation rate in Scenario A (Fig. 5). It was found that both the maximum formation rate and the percentage of water conversion increased with the space between the two packings but the overall degree of increment was not obvious (< 15%).

These results demonstrated that it was possible to effectively facilitate the hydrate nucleation by changing the relative positions of the packings. However, it remained

unclear whether the observed improvement on the nucleation was mainly attributed to the relative distance between the two packings or the relative distance between the packings and the gas-water interface. As shown in Fig. 1, both packings were completely immersed in the 200 mg L^{-1} αCD - 100 mg L^{-1} SDS mixture solution in Scenario A. In this case, there was about 5 mm thick water column between the gas-water interface and the top of the two packings. In Scenario B, the bottom surface of the top packing was located at the gas-water interface. By contrast, the top packing was completely exposed in the methane gas phase in Scenario C. It was speculated that the top packing above the gas-water interface was critical for the hydrate nucleation while the bottom packing immersed in liquid contributed little to the facilitated nucleation. As shown in Fig. 6a, methane hydrates were only observed at the top packing while little hydrates were formed at the bottom packing in Scenario C.

Effect of relative position between packing and gas-water interface on hydrate formation: In order to validate the above speculation and reveal the effects of the relative position between packing and gas-water interface on hydrate formation, we added experiments by removing the bottom packing and placing only the top packing located at L_2 (Scenario D), L_3 (Scenario E) and L_4 (Scenario F), respectively. In these cases, the mass ratio of packing to water was 35%.

Results indicated that the induction time for hydrate nucleation was 47 h in Scenario D which was more than twice of that in Scenario A (Fig. 5). It was interesting to observed that the induction time was 5.4 h and 6.0 h in Scenario E and F, respectively, which was

76% and 73% less than that in Scenario A. This finding confirmed that it was the packing exposed to the gas phase rather than the packing immersed in the aqueous phase that indeed contributed to the faster nucleation. Moreover, the rate of hydrate growth increased with the hight of the packing's position. For example, the maximum formation rate increased from 6.4 to 7.0 and 7.8 m^3 gas m^{-3} water min^{-1}, respectively, when the packing moved from L_2 to L_3 and L_4 (Fig. 4). The percentage of water conversion also increased from 51% at L_2 to 69% at L_3 and 79% at L_4, respectively (Fig. 3).

Neverthess, the application of only one packing remained inadequate for successful gas storage because the hydrate nucleation was still two-order of magnitude slower than the reaction under stirring conditions using the same concentration of αCD-SDS mixture solution (Tian and Wu, 2020a). Additionally, the percentage of water conversion decreased when the mass ratio of packing to water decreased from 70% to 35%, especially when the top packing was located at L_2 or L_3 (Fig. 3).

Location optimization for SFC packings: Accroding to the above results, we added another three experimental scenarios (Scenario G – I) by using two packings again aiming to find out an optimized location pattern of the packings. As shown in Figs. 1g - 1i, at least one packing was located above the gas-water interface while the other packing was placed at L_2 or L_3 instead of L_1.

In Scenario G, the two packings were located at L_2 and L_3, respectively, which resulted in a final gas uptake of 128.0 mmol gas mol^{-1} water (Fig. 2) and 78% of the initial water was converted into hydrate (Fig. 3). These two parameters were about 5% higher than

that in Scenario A, while the induction time (4.88 h) was only about 20% of that in Scenario A. Subsequently, both packings were moved upwards to L_3 and L_4, respectively, without changing the vertical distance between them (Scenario H). In this case, all packings were in the gasous phase as the bottom surface of the packings was 2 mm above the gas-water interface. Methane hydrates were observed inside the pores of both packings, but there was a hollow region below the bottom packings in the reactor where hydats were not observed (Fig. 6b). Compared with Scenario G, such location pattern led to little difference in the total gas uptake and the percentage of water conversion, but the induction time (0.33 h) could be effectively reduced by 93% (Fig. 5). The time required for hydrate nucleation in this case was only less than 2% of that in Scenario A. It was also observed that a larger distance between the two packings did not guarantee a better performance. For example, the induction time increased by one order of magnitude while the percentage of water conversion decreased by about 6% if the bottom packing was moved from L_3 (gas phase) to L_2 (aquesous phase) as shown in Scenario I.

It was noted that the standard devisions of the induction time (error bars) were relatively big in some scenarios such as Scenarios A, B, C, D, E (Fig. 5). Therefore, we added three more parallel experiments for each of these 5 scenarios. To evaluate if it would impact the conclusion that Scenario H was the optimal location pattern with the best hydrate formation performance, we also added three more parallel experiments for Scenario H although the error bar from 3 trials was small. Accordingly, we totally had 6 independent trials for each scenario and then compared the results with that obtained from 3 trials.

Results demonstrated that the overall tendency did not change after 6 trials. The shortest induction time was still observed in Scenario H where the error bar remained small, which suggested that the hydrate nucleation was relatively stable in this case (Fig. S1 in the Supporting Information). However, the error bars of induction time in the other five scenarios remained big and the deviation was not significantly reduced after adding more trials. These results suggested that the relatively big error bars might be associated with the stochastic nature of hydrate nucleation which had been previously reported especially under unstirred conditions. This fact became one of the challenges for the stable operation of gas storage technology based on hydrate formation. Our results indicated that both the average value and the standard deviation of the induction time could be minimized by optimizing the location of ceramic packings using the packing tray reactor.

Moreover, it should be noted that the effects from the stainless-steel reactor internal could not be ignored, because our previous studies demonstrated that the metal internals such as coiled metal tubes (Pang et al., 2007) and stainless-steel meshes (Hu et al., 2019) could also promote hydrate formation. In the conext of this study, our results highlighted the predominant role of the SFC packings during the hydrate nucleation stage. To better clarify this, we repeated the experiments by adding the αCD-SDS mixture solution and the stainless-steel reactor internal but not adding SFC packings. In this case, hydrate nucleation was only observed in one of the five runs in absence of SFC packings (induction time: 48.5 h). When the reaction transited from nucleation to fast growth stage, the fast gas uptake might result from combination effects from the stainless-steel reactor

internal and the SFC packings especially in the cases when the packings were located above the gas-water interface (e.g., Scanario F).

Another important finding was that the porous packings should be located at the gas phase near the gas-water interface rather than immersed in the aqueous phase. This was a little suprising as the water inside the packings in the gas phase might be inadequate for hydrate nucleation, therefore, there should be some mechanisms that contributed to pump water from the aqueous phase to the packings' pores to induce and maintain reaction. To better elaborate this process, a schematic is shown in Fig. 7.

Before reaction, water might climb along the stainless-steel reactor internal and the inner wall of the reactor and subsequently move along the tortuous pathways inside the packings' pores driven by the capillary force (Fig. 7a), which had been reported in previous studies (Linga et al., 2012; Babu et al., 2013a; Hu et al., 2018). This resulted in an unsaturated porous environment inside the packings, which was supposed to be more favorable for hydrate formation compared with the saturated packing soaked in water, because the decrease in pore water content might provide more free passages for gas, facilitate water transport and enhance mass transfer by providing larger gas-water contact area for reaction (Xie et al., 2020). This could be supported by previous studies on the hydrate formation dynamics in porous media. For example, Bagherzadeh et al. (2011) observed more spatially uniform and faster hydrate formation in silica sands with lower initial moisture content. Badu et al. (2013a) also demonstrated that the gas uptake, hydrate growth rate and water conversion to hydrates increased significantly as the water

saturation in the silica sand bed decreased from 100% to 50%.

At early stage of nucleation, hydrate film formed at the gas-water interface which might also contribute to the water migration uptowards the packings, because the formed hydrate would cause intense suction force and adsorb the surrounding water due to the lower Gibbs free energy on the hydrate surface (Sloan and Koh, 2007). The water adsorption phenomenon had been visually observed in a one-dimensional reactor (Chen et al., 2017) and experimentally detected by the pF-meter sensors in porous media (Zhang et al., 2010a; Zhang et al., 2010b). It should be noted that the gas-water interface in this study exsited at the top surface of the bulk water or at the surface of the pore water trapped inside the unsaturated packings. At the interface between the gas and the top surface of bulk water, the hydrate clusters served as "bridge" to assist the transport of water to the bottom of the SFC packing which was then lifted by the upward capillary force and entered the pores (Fig. 7a). At the interface between the gas and the pore water, porous hydrate shell would form on the surface of water droplet in the pore. According to Liang et al. (2022), the continual outward transport of water through the hydrate shell caused the hydrate shell thickening, while the mass transfer of water was initially controlled by diffusion and then transformed into permeation. Meanwhile, the hydrate clusters coated on the inner surface of the backbone framework of the SFC packing would grow to a thick layer and eventually formed a hydrate film network (Fig. 7b). According to Chen et al. (2017), the hydrate formation and water adsorption could occur intermittently and eventually form hydrate film network inside the porous materials. Another driving force

for the migration of water towards packings' pores might be attributed to role of the αCD - SDS mixture solution used in this study (Fig. 7c). It is known that the cyclodextrins and SDS would form channel-type dimers and the H-bonds between each two dimers would form a fully hydrophilic zone at the gas-water interface, which had been proven to be able to promote the upward movement of water (Hernández-Pascacio et al., 2007).

From the above discussion, we believed that there were synergistic effects between the capillary force from the porous packings and the water suction force from the initially formed hydrate clusters which pumped water into the packings' pores. Our results highlighted the role of such effects for enabling hydrate nucleation in the unsaturate pores exposed in gas phase. However, it didn't mean we could conclude that porous packings with higher capillary performance would be better, because the distribution of the pore water was inhomogeneous while a strong capillary force would draw the water away from the hydrate film to the pores with less moisture content (Yin et al., 2016). This process might be adverse for hydrate nucleation by destroying the initially formed hydrate film structure and hindering the aggregation of hydrate clusters to form larger crystals. To validate this speculation, we repeated the experiments in Scenarios G and H using the customized SFC packings with the same pore size (3 ~ 5 mm) but with larger porosity, which was expected to have more pore numbers and relatively stronger capillary performance (Lee et al., 2019). A decreased gas uptake was observed when the packing's porosity increased from 60% to 79% (Fig. 8). Results also confirmed that the hydrate nucleation in presence of SFC packings with large porosity was one-order of magnitude

slower than that with small porosity in Scenario H (Fig. 9b). It appeared that the increase in the porosity mainly influence the hydrate formation kinetics during the initial nucleation stage rather than the fast growth stage because the decrease in the maximum formation rate was very slight (Fig. 9b). Similar tendency was observed in Scenaro G (Fig. 9a).

Effect of pressure on hydrate formation when packings were located at the gas phase:

In order to study the hydrate formation behavior under different pressures, the experiments in Scenarios G and H which were demonstrated as most effective location patterns were repeated at 7 MPa and 6 MPa using 60% and 79% porosity SFC packings, respectively. When SFC porosity was 60%, the gas uptake decreased by about 20% when the pressure decreased from 8 MPa to 7 MPa, which further decreased by about 30% when the pressure decreased to 6 MPa in both Scenario G and H (Fig. 10a). Although the difference in the final gas uptake was negligible in Scenario G and H at the same pressure, the hydrate nucleation showed obvious inconsistency. The induction time increased from 4.88 h to 8.35 h when the pressure decreased from 8 MPa to 7 MPa in Scenario G. However, the fast hydrate nucleation was observed at 7 MPa as the induction time was only 0.28 h in Scenario H, indicating this packing location pattern was more favorable for gas hydrate nucleation (Fig. 11a). The hydrate formation could not be efficiently promoted at 6 MPa as the induction time were longer than 10 h and the gas uptake were only about 70 mmol gas mol^{-1} water in both Scenarios. When the porosity of SFC packing was 79%, the final gas uptake was in the range of 100 - 110 mmol gas mol^{-1} water at 7

and 8 MPa in both Scenaris. However, the hydrate formation showed significant hysteresis in Scenario G compared with Scenario H at the same pressure. For example, the amount of gas uptake reached 100 mmol gas mol^{-1} water at 25 min in Scenario G at 8 MPa, but such time was 200 min in Scenario G. Similarly, the amount of gas uptake reached 90 mmol gas mol^{-1} water at 50 min in Scenario G at 7 MPa, such time increased to about 125 min in Scenario G (Fig. 10b). Despite a shorter induction time (7.94 h) at 7 MPa when the porosity was 79% compared to 60% in Scenario G, such value exceeded 10 h in Scenario H at the same pressure. The above results demonstrated that the packing location pattern in Scenario H was optimal with the fast hydrate nucleation at 7 and 8 MPa, but a higher SFC packing porosity didn't aid the hydrate formation.

4. Conclusions

This study demonstrated that the usage of the αCD-SDS mixture solution alone could not effectively induce methane hydrate nucleation under unstirred conditions, while the addition of SiC foam trays in the reactor could successfully induce hydrate nucleation in the αCD-SDS mixture solution. However, the average induction time was 670 times longer than that with mechanical agitation if all SFC packings were immersed in the aqueous phase. The hydrate formation could be significantly facilitated by optimizing the positions of the SiC foam trays under unstirred conditions. The most pronounced improvent was observed when all the SFC packings were exposed in the gaseous phase near the gas-water interface, which could decrease the hydrate induction time from 22.3

h to 0.33 h. The maximum formation rate and the percentage of water conversion to hydrates after optimization differed insignificantly with that obtained under mechanical agitation. Such improvement was mainly attributed to the formation of unsaturated porous environment inside the packings which was more favorable for hydrate formation compared with the saturated packing soaked in water. Results also suggested that the hydrate formation was induced and maintained by pumping water from the aqueous phase to the pores, which was driven by several processes such as the capillary force from the porous packings, water adsorption from the hydrate clusters at the gas-water interface and from the hydrate film network at the inner surface of the packings' pores, and the water channels formed by the αCD-SDS dimers at the gas-water interfaces.

Acknowledgements

This study was financially supported by Shenzhen Science and Technology Program (No. GJHZ20200731095600002, No. JCYJ20210324140810027), International Joint Research Funding from Shenzhen International Graduate School of Tsinghua University (No. HW 2020011), and Stable Support Funding from the Science, Technology and Innovation Commission of Shenzhen Municipality (No. WDZC20200818183253001).

References

Babu, P., Kumar, R., Linga, P., 2013a. Medium pressure hydrate based gas separation (HBGS) process for pre-combustion capture of carbon dioxide employing a novel fixed bed reactor. Int J Greenh Gas Con 17, 206-214.

Babu, P., Kumar, R., Linga, P., 2013b. A new porous material to enhance the kinetics of clathrate process: application to precombustion carbon dioxide capture. Environ Sci Technol 47, 13191-13198.

Bagherzadeh, S.A., Moudrakovski, I.L., Ripmeester, J.A., Englezos, P., 2011. Magnetic Resonance Imaging of Gas Hydrate Formation in a Bed of Silica Sand Particles. Energ Fuel 25, 3083-3092.

Bhattacharjee, G., Goh, M.N., Arumuganainar, S.E.K., Zhang, Y., Linga, P., 2020. Ultra-rapid uptake and the highly stable storage of methane as combustible ice. Energ Environ Sci 13, 4946-4961.

Chen, L.-T., Li, N., Sun, C.-Y., Chen, G.-J., Koh, C.A., Sun, B.-J., 2017. Hydrate formation in sediments from free gas using a one-dimensional visual simulator. Fuel 197, 298-309.

Fan, S., Yang, L., Lang, X., Wang, Y., Xie, D., 2012. Kinetics and thermal analysis of methane hydrate formation in aluminum foam. Chem Eng Sci 82, 185-193.

Hernández-Pascacio, J., Garza, C., Banquy, X., Díaz-Vergara, N., Amigo, A., Ramos, S., Castillo, R., Costas, M., Piñeiro, Á., 2007. Cyclodextrin-Based Self-Assembled Nanotubes at the Water/Air Interface. J Phys Chem B 111, 12625-12630.

Hu, P., Chen, D., Zi, M., Wu, G., 2018. Effects of carbon steel corrosion on the methane hydrate formation and dissociation. Fuel 230, 126-133.

Hu, P., Wu, G., Zi, M., Li, L., Chen, D., 2019. Effects of modified metal surface on the formation of methane hydrate. Fuel 255, 115720.

IEA, 2017. World Energy Outlook 2017.

Ji, H., Chen, D., Wu, G., 2017. Molecular mechanisms for cyclodextrin-promoted methane hydrate formation in water. J Phys Chem C 121, 20967-20975.

Lee, J., Suh, Y., Dubey, P.P., Barako, M.T., Won, Y., 2019. Capillary Wicking in Hierarchically Textured Copper Nanowire Arrays. ACS Appl Mater Inter 11, 1546-1554.

Liang, H., Guan, D., Shi, K., Yang, L., Zhang, L., Zhao, J., Song, Y., 2022. Characterizing Mass-Transfer mechanism during gas hydrate formation from water droplets. Chem Eng J 428, 132626.

Linga, P., Clarke, M.A., 2017. A Review of Reactor Designs and Materials Employed for Increasing the Rate of Gas Hydrate Formation. Energ Fuel 31, 1-13.

Linga, P., Daraboina, N., Ripmeester, J.A., Englezos, P., 2012. Enhanced rate of gas hydrate formation in a fixed bed column filled with sand compared to a stirred vessel. Chem Eng Sci 68, 617-623.

Liu, X., Tian, L., Chen, D., Wu, G., 2019. Accelerated formation of methane hydrates in the porous SiC foam ceramic packed reactor. Fuel 257, 115858.

Messina, C.M., Faggio, C., Laudicella, V.A., Sanfilippo, M., Trischitta, F., Santulli, A.,

2014. Effect of sodium dodecyl sulfate (SDS) on stress response in the Mediterranean mussel (Mytilus Galloprovincialis): Regulatory volume decrease (Rvd) and modulation of biochemical markers related to oxidative stress. Aquat Toxicol 157, 94-100.

Pang, W.X., Chen, G.J., Dandekar, A., Sun, C.Y., Zhang, C.L., 2007. Experimental study on the scale-up effect of gas storage in the form of hydrate in a quiescent reactor. Chem Eng Sci 62, 2198-2208.

Qian, J.M., Jin, Z.H., 2006. Preparation and characterization of porous, biomorphic SiC ceramic with hybrid pore structure. J Eur Ceram Soc 26, 1311-1316.

Sloan, E.D., Koh, C.A., 2007. Clathrate hydrates of natural gases. CRC press.

Tian, L., Wu, G., 2020a. Cyclodextrins as promoter or inhibitor for methane hydrate formation? Fuel 264, 116828.

Tian, L., Wu, G., 2020b. Thermal analysis of methane hydrate formation in a high-pressure reactor packed with porous SiC foam ceramics. Fuel 260, 116307.

Veluswamy, H.P., Kumar, A., Seo, Y., Lee, J.D., Linga, P., 2018. A review of solidified natural gas (SNG) technology for gas storage via clathrate hydrates. Appl Energ 216, 262-285.

Wang, F., Song, Y., Liu, G., Guo, G., Luo, S., Guo, R., 2018. Rapid methane hydrate formation promoted by Ag&SDS-coated nanospheres for energy storage. Appl Energ 213, 227-234.

Xie, Y., Li, R., Wang, X.-H., Zheng, T., Cui, J.-L., Yuan, Q., Qin, H.-B., Sun, C.-Y.,

Chen, G.-J., 2020. Review on the accumulation behavior of natural gas hydrates in porous sediments. J Nat Gas Sci Eng 83, 103520.

Yan, P., Li, X., Li, H., Gao, X., 2018. Hydrodynamics and flow mechanism of foam column Trays: Contact angle effect. Chem Eng Sci 176, 220-232.

Yang, L., Fan, S., Wang, Y., Lang, X., Xie, D., 2011. Accelerated formation of methane hydrate in aluminum foam. Ind Eng Chem Res 50, 11563-11569.

Yin, S.-h., Wang, L.-m., Chen, X., Wu, A.-x., 2016. Effect of ore size and heap porosity on capillary process inside leaching heap. T Nonferr Metal Soc 26, 835-841.

Zhang, L., Liu, X., Li, H., Sui, H., Li, X., Zhang, J., Yang, Z., Tian, C., Gao, G., 2012. Hydrodynamic and Mass Transfer Performances of a New SiC Foam Column Tray. Chem Eng Tech 35, 2075-2083.

Zhang, L., Liu, X., Li, X., Gao, X., Sui, H., Zhang, J., Yang, Z., Tian, C., Li, H., 2013. A Novel SiC Foam Valve Tray for Distillation Columns. Chinese J Chem Eng 21, 821-826.

Zhang, P., Wu, Q., Jiang, G., Zhan, J., Wang, Y., 2010a. Water transfer characteristics in the vertical direction during methane hydrate formation and dissociation processes inside non-saturated media. J Nat Gas Chem 19, 139-145.

Zhang, P., Wu, Q., Pu, Y., Jiang, G., Zhan, J., Wang, Y., 2010b. Water transfer characteristics during methane hydrate formation and dissociation processes inside saturated sand. J Nat Gas Chem 19, 71-76.

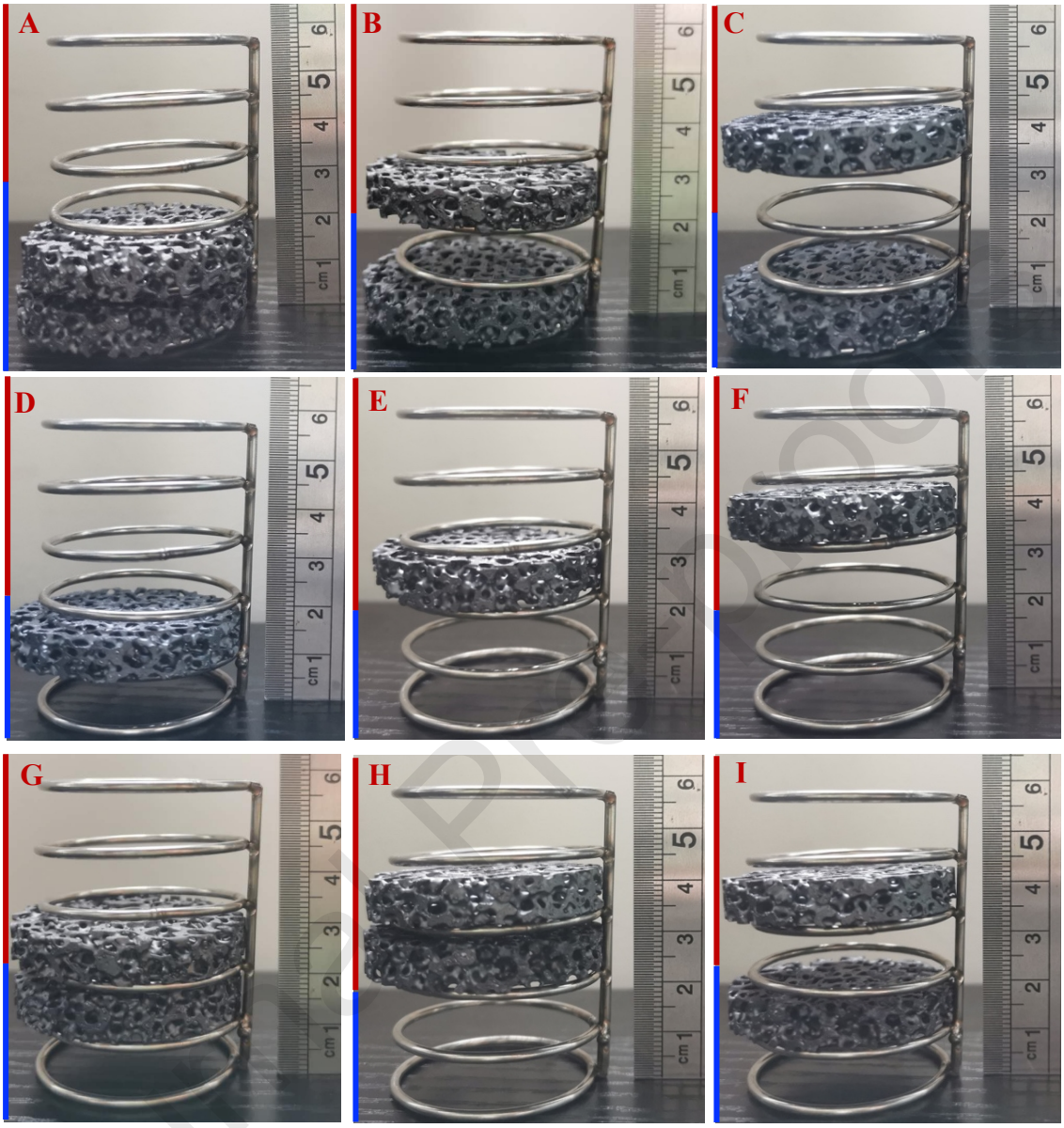

Fig. 1 Experimental scenarios with SFC packings located at different positions in the packing trays reactor. The blue bars show the height of the aqueous phase inside the reactor. A to I show the Scenario A to Scenario I, respectively.

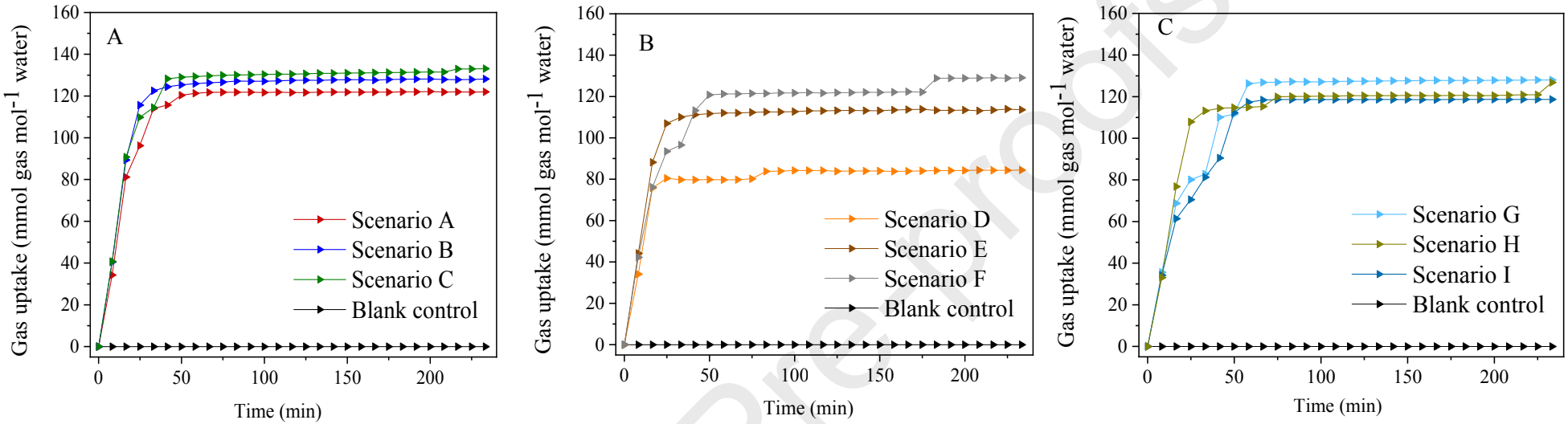

Fig. 2 Gas uptake during methane hydrate formation in different experimental scenarios

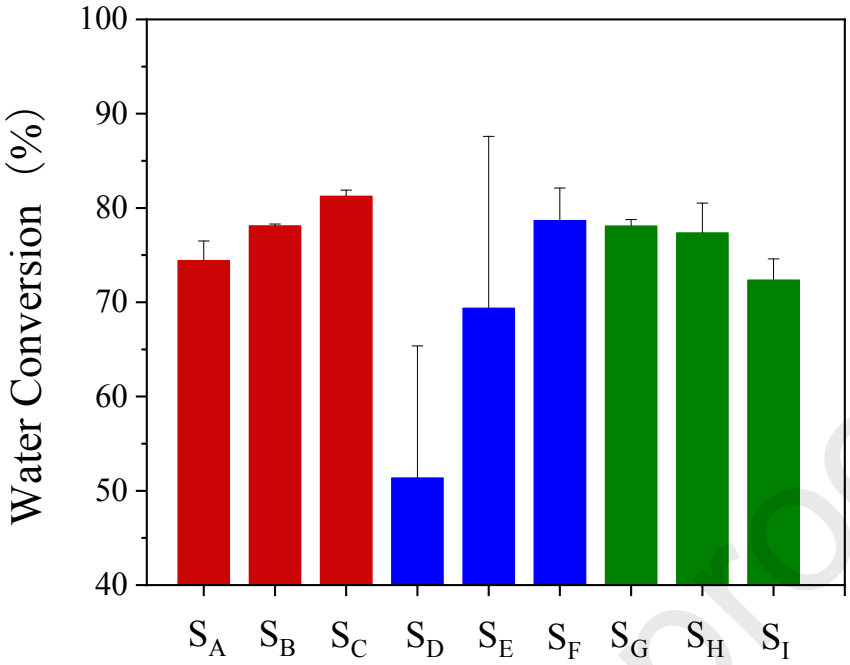

Fig. 3 Percentage of water conversion to hydrates during methane hydrate formation in different experimental scenarios. S_A to S_I represent Scenario A to Scenario I.

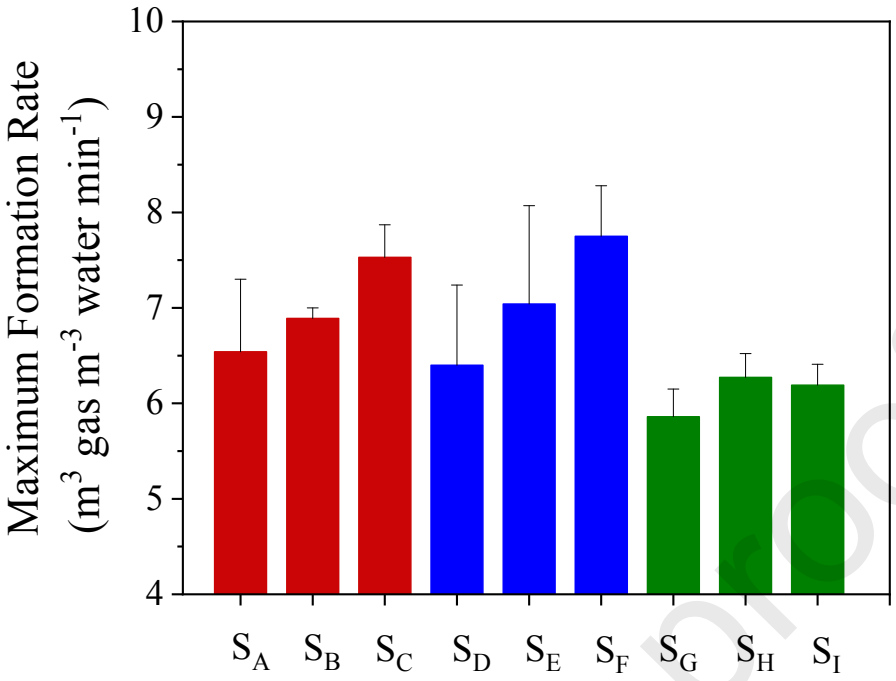

Fig. 4 Maximun formation rate during methane hydrate formation in different experimental scenarios. S_A to S_I represent Scenario A to Scenario I.

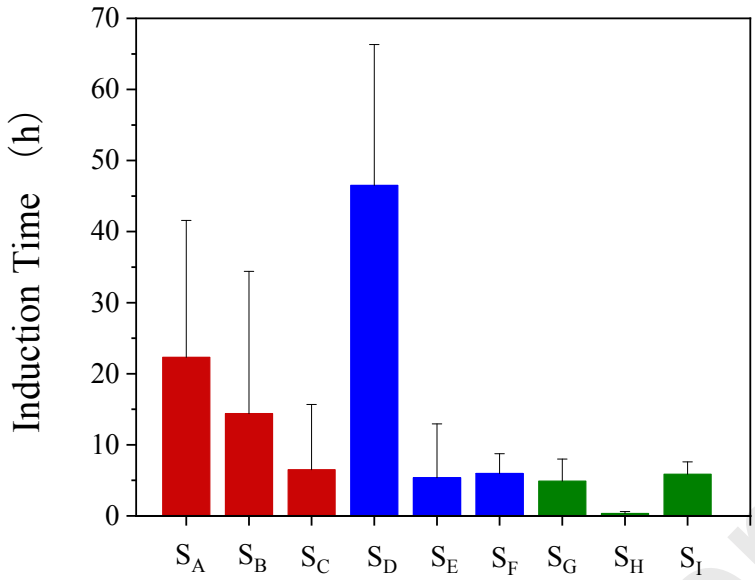

Fig. 5 Induction time during methane hydrate formation in different experimental scenarios. S_A to S_I represent Scenario A to Scenario I.

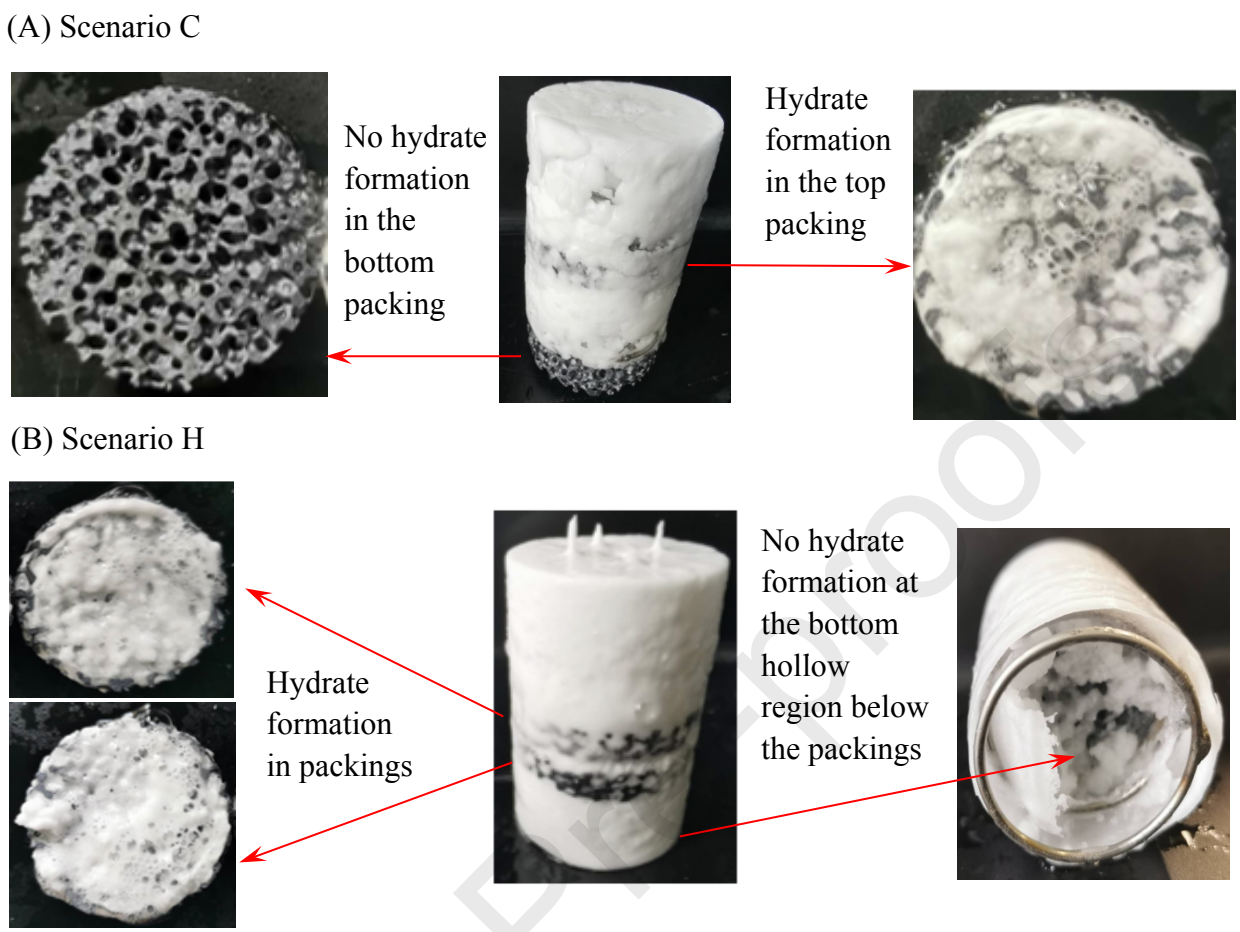

Fig. 6 Pictures showing the formation of methane hydrate at different regions in the SiC foam tray reactor

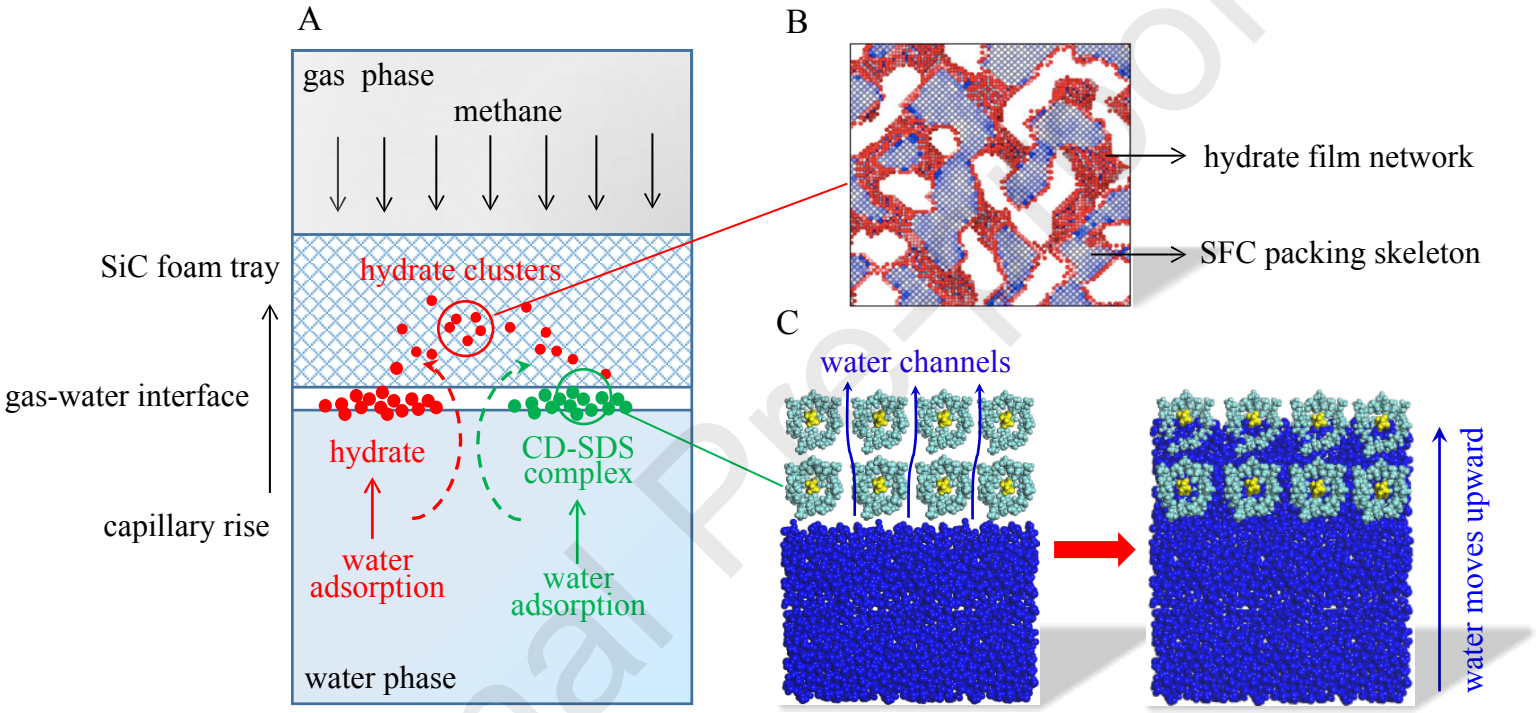

Fig. 7 Schematic showing the drving forces for water migration and hydrate formation in presence of SFC packings at the gas-water interface

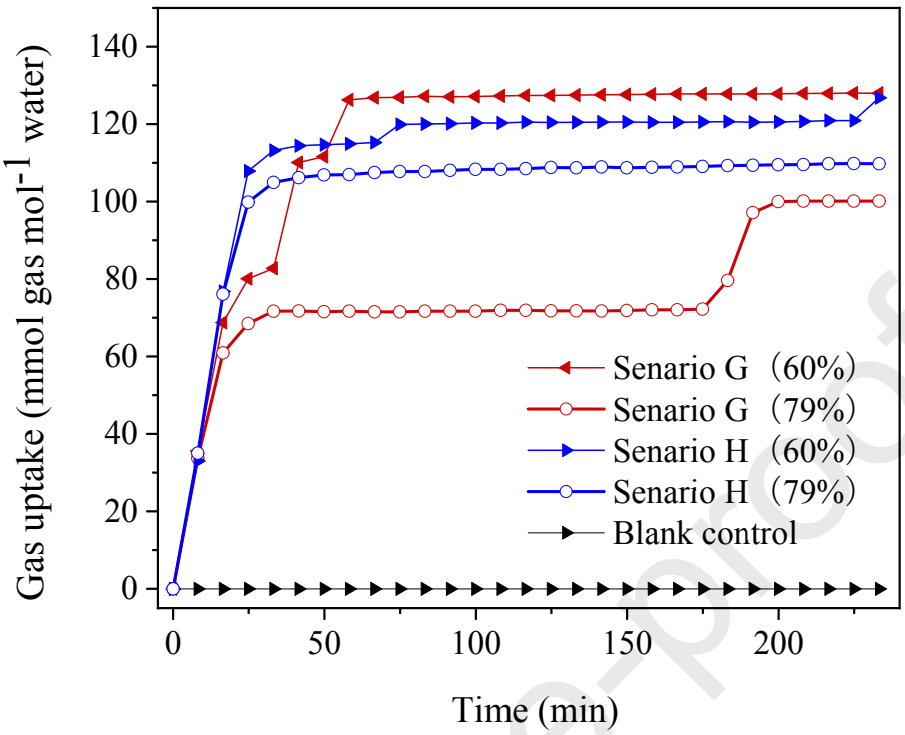

Fig. 8 Changes in the gas uptake during methane hydrate formation when the SFC porosity increased from 60% to 79%

(A) Scenario G

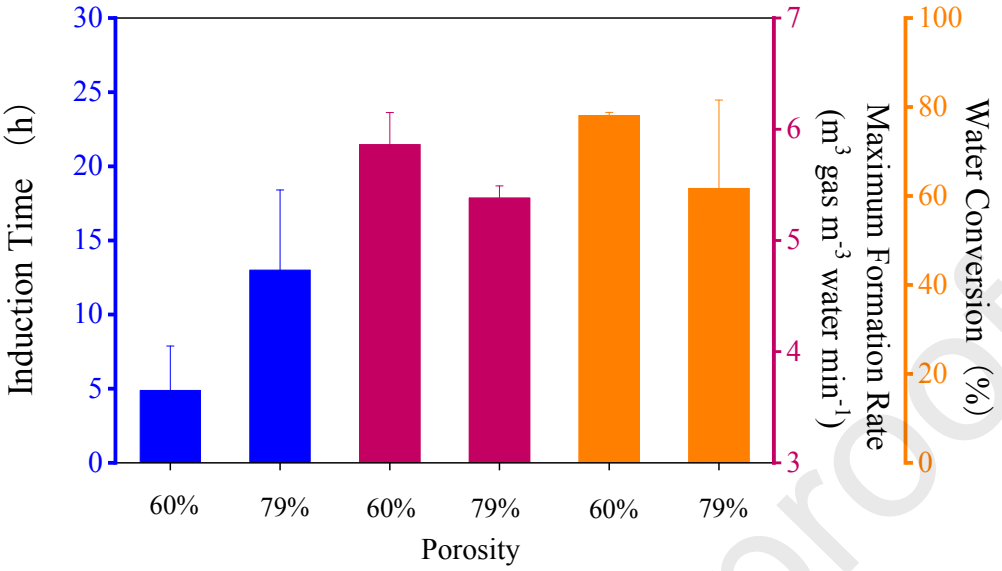

(B) Scenario H

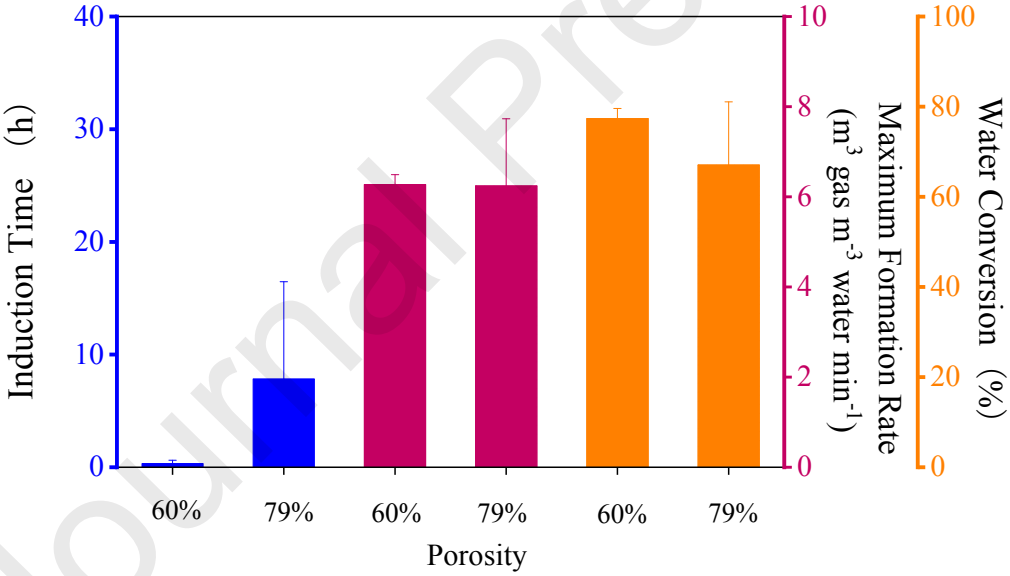

Fig. 9 Changes in the induction time, maximum formation rate and percentage of water conversion to hydrate during methane hydrate formation when the SFC porosity increased from 60% to 79%

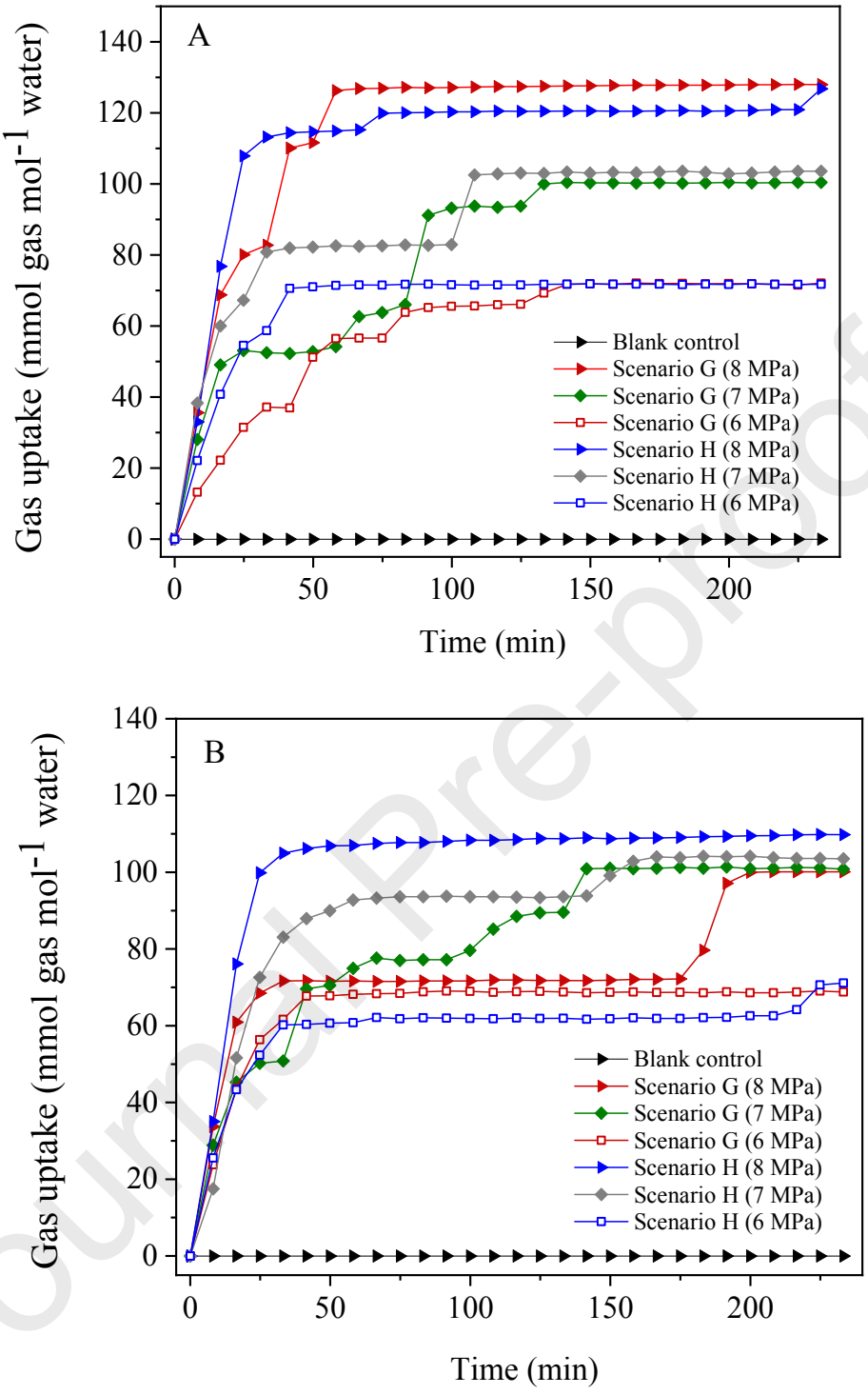

Fig. 10 Changes in the gas uptake during methane hydrate formation at different pressures when SFC porosity was (A) 60% and (B) 79%

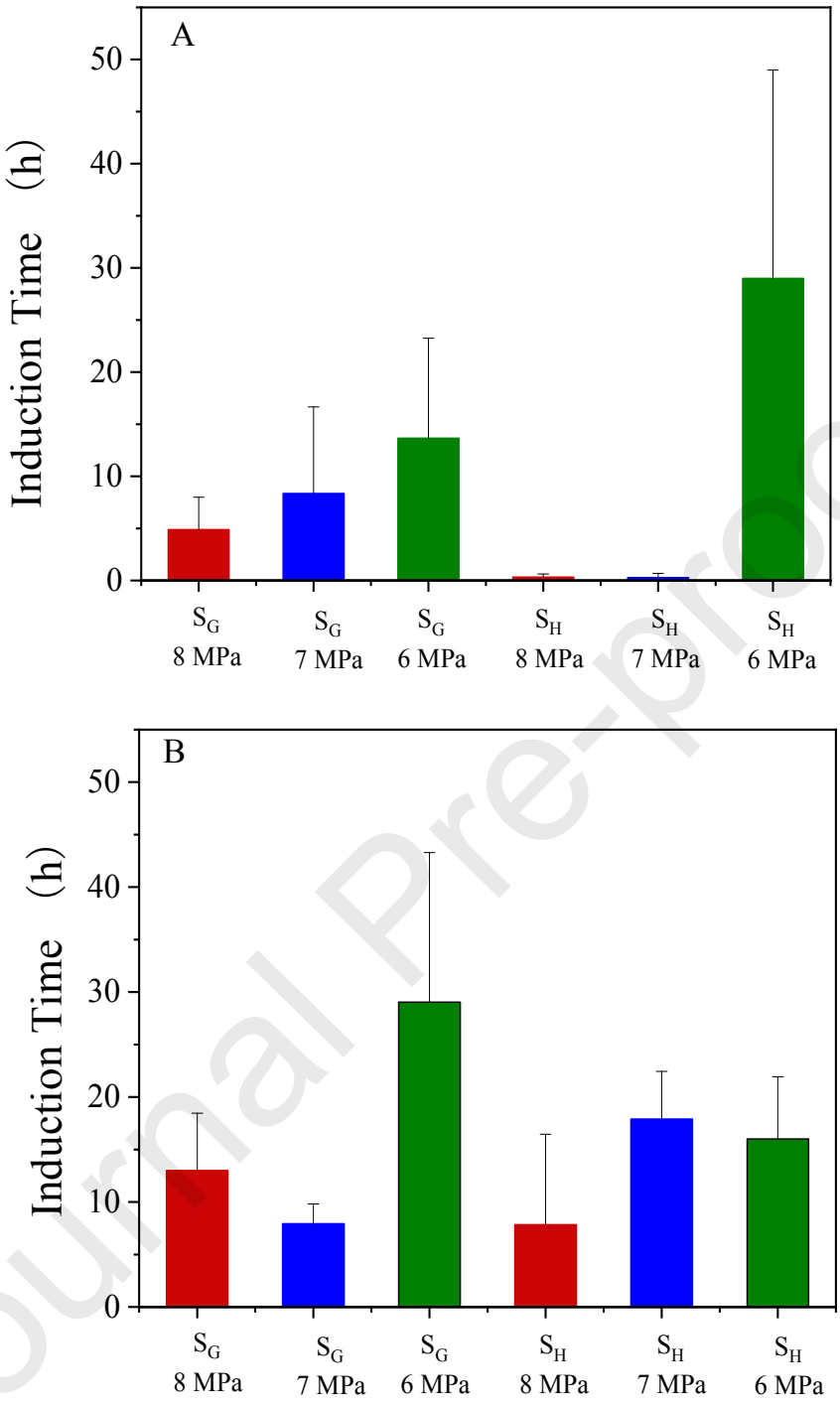

Fig. 11 Changes in the induction time at different pressures when the SFC porosity was (A) 60% and (B) 79%. S_G and S_H represent Scenario G and Scenario H

CRediT Author Statement

Linqing Tian: Conceptualization, Methodology, Experiments, Validation, Data Analysis, Writing-Review & Editing. **Li Ha**: Experiments. **Li Wang**: Experiments. **Guangjin Chen**: Writing-Review & Editing. **Frederic Coulon:** Project administration, Writing-Review & Editing. **Yuelu Jiang**: Writing-Review & Editing. **Xinyang Zeng:** Writing-Review & Editing. **Ruifeng Zhang**: Project administration. **Guozhong Wu**: Conceptualization, Writing-Review & Editing, Supervision, Project administration, Funding acquisition.

Declaration of interests

☒ The authors declare that they have no known competing financial interests or personal relationships that could have appeared to influence the work reported in this paper.

☐The authors declare the following financial interests/personal relationships which may be considered as potential competing interests:

Graphical Abstract

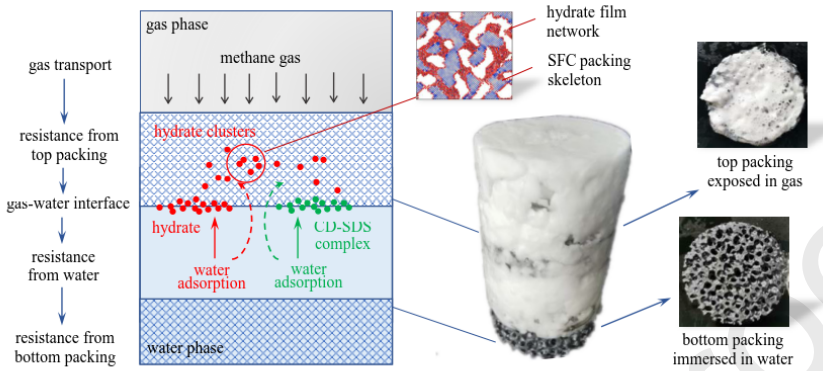

Highlights

- SiC foam tray reactor was for the first time used to enhance gas hydrate formation
- Foam packings should be located at the gas phase near the gas-water interface
- Stochastic hydrate nucleation time was stabilized by optimizing packing's location